1   # DENSITY DEPENDENCE IN DEMOGRAPHY AND DISPERSAL GENERATES

2   # FLUCTUATING INVASION SPEEDS

3   Lauren L. Sullivan[a,1], Bingtuan Li[b], Tom E. X. Miller[c], Michael G. Neubert[d],

4   Allison K. Shaw[a,1]

5   [a]Department of Ecology, Evolution and Behavior, University of Minnesota, Saint

6   Paul, MN 55108; [b]Department of Mathematics, University of Louisville, Louisville,

7   KY 40292; [c]Department of Ecology and Evolutionary Biology, Rice University,

8   Houston, TX 77005; [d]Biology Department, Woods Hole Oceanographic Institution,

9   Woods Hole, MA 02543

10   Author Contributions: T.E.X.M., M.G.N., and A.K.S. designed initial research;

11   L.L.S. and M.G.N. led simulations; L.L.S. led writing; All authors contributed to

12   ideas development and writing.

13   [1]To whom correspondence should be addressed. Email: lsulliva@umn.edu, or

14   ashaw@umn.edu

Abstract

Density dependence plays an important role in population regulation and is known to generate temporal fluctuations in population density. However, the ways in which density dependence affects spatial population processes, such as species invasions, are less understood. While classical ecological theory suggests that invasions should advance at a constant speed, empirical work is illuminating the highly variable nature of biological invasions, which often exhibit non-constant spreading speeds even in simple, controlled settings. Here, we explore endogenous density dependence as a mechanism for inducing variability in biological invasions with a set of population models that incorporate density dependence in demographic and dispersal parameters. We show that density dependence in demography at low population densities—i.e., an Allee effect—combined with spatiotemporal variability in population density behind the invasion front can produce fluctuations in spreading speed. The density fluctuations behind the front can arise from either overcompensatory population growth or from density-dependent dispersal, both of which are common in nature. Our results demonstrate that simple rules can generate complex spread dynamics, and highlight a novel source of variability in biological invasions that may aid in ecological forecasting.

Introduction

Fluctuations in population size have long fascinated ecologists and fueled a now-classic debate over whether populations are governed by extrinsic environmental factors or by intrinsic self-limitation (15). One of the most important advances of twentieth-century ecology was the discovery that intrinsic density feedbacks can cause population densities to fluctuate, even in constant environments (26; 5; 48). This discovery helped resolve the important role of density dependence in population regulation, revealing that strong regulating forces can generate dynamics superficially consistent

⁴² with no regulation at all. Our understanding of temporal fluctuations in population

⁴³ size stands in sharp contrast with our relatively poor understanding of fluctuations

⁴⁴ in the spatial dimension of population growth: spread across landscapes.

⁴⁵ Understanding the dynamics of population spread takes on urgency in the current

⁴⁶ era of human-mediated biological invasions and range shifts in response to climate

⁴⁷ change. The velocity of spread, or "invasion speed", is a key summary statistic of an

⁴⁸ expanding population and an important tool for ecological forecasting (8). Estimates

⁴⁹ of invasion speed are often derived from regression methods that describe change

⁵⁰ in spatial extent with respect to time (30; 1; 49). Implicit in this approach is the

⁵¹ assumption that the true spreading speed is constant and deviations from it represent

⁵² "error" in the underlying process, or in human observation of the process. This

⁵³ assumption is reinforced by long-standing theoretical predictions that, under a wide

⁵⁴ range of conditions, a population will asymptotically spread with a constant velocity.

⁵⁵ Invasion at a constant speed can arise from both *pulled* waves (where the advancing

⁵⁶ wave moves forward by dispersal and rapid growth of low-density populations far

⁵⁷ in front of the advancing wave (56; 44; 16; 32)), as well as *pushed* waves (where the

⁵⁸ invasion is driven by reproduction and dispersal from high-density populations behind

⁵⁹ the invasion front (21; 55; 50)). The conventional wisdom of a long-term constant

⁶⁰ invasion speed is widely applied (53; 9).

⁶¹ In contrast to classic approaches that emphasize a long-term constant speed, there

⁶² is growing empirical recognition that invasion dynamics can be highly variable and

⁶³ idiosyncratic (27; 29; 34; 59; 60; 4; 54; 14). There are several theoretical explanations

⁶⁴ for fluctuations in invasion speed (which we define here as any persistent tempo-

⁶⁵ ral variability in spreading speed), including stochasticity in either demography or

⁶⁶ dispersal (35; 54; 17; 42; 14), and temporal or spatial environmental heterogeneity

⁶⁷ (43; 33; 57; 58; 3; 40). Indeed, empirical studies often attribute temporal variation

⁶⁸ in speed to differences in the environments encountered by the invading population

3

69 (e.g., (1; 37)). Predator-prey dynamics can also induce fluctuating invasion speeds

70 (33; 7). Notably, Dwyer and Morris (7) showed that density feedbacks can produce

71 fluctuations in spreading speed, yet we still have an incomplete understanding of the

72 conditions under which fluctuations in speed arise. Surprisingly few theoretical stud-

73 ies have since investigated these density feedbacks, especially with respect to their

74 effect on endogenously-driven speed fluctuations, despite recent empirical work on

75 invasion variability (34; 59; 53; 60).

76   Here, we develop deterministic, single-species mathematical models of spatial

77 spread to ask under what conditions the invasion speed of an expanding popula-

78 tion can fluctuate in a spatially uniform and temporally constant environment. As

79 a starting point, we took inspiration from the relatively complete understanding of

80 fluctuations in population size generated by density dependence in nonspatial mod-

81 els (48). We conjectured that density-dependent feedbacks might similarly generate

82 fluctuating invasion speeds pursuing the suggestion first made in (7). Because spread

83 dynamics are jointly governed by demography (local births and deaths) and dispersal

84 (spatial redistribution), we considered several types of density feedbacks (39), in-

85 cluding positive density dependence in population growth (i.e., Allee effects) at the

86 low-density invasion front (47), and density-dependent movement (25; 7).

87   Our analysis uncovered novel density-dependent mechanisms that can induce vari-

88 ability in invasion speed, with fluctuations ranging from stable two-point cycles to

89 more complicated aperiodic dynamics. By demonstrating that simple invasion mod-

90 els can generate complex spread dynamics, our results reveal previously undescribed

91 sources of variability in biological invasions and provide a roadmap for empirical

92 studies to detect these processes in nature.

4

Models and Results

$_{94}$ We use integrodifference equations (16) to model population growth and spread.

$_{95}$ These models describe the change in population density $(n_t(x))$ from time t to time

$_{96}$ $t+1$ as the result of demography and dispersal. First, individuals at location y gen-

$_{97}$ erate $f(n_t(y))$ offspring and then die. Next, a fraction p of these offspring disperse.

$_{98}$ The probability that a dispersing individual moves from location y to location x is

$_{99}$ given by the dispersal kernel, $k(x-y)$. The remaining fraction $(1-p)$ remain at their

$_{100}$ natal location. Concatenating reproduction and dispersal, we have (51; 52; 22; 23):

$$n_{t+1}(x) = (1-p)f\big(n_t(x)\big) + \int_{-\infty}^{\infty} p\, k(x-y)f\big(n_t(y)\big)\, dy. \tag{1}$$

$_{101}$ We will assume that $f(1) = 1$, so that the population has an equilibrium at the

$_{102}$ carrying capacity $n_t(x) = 1$, and that the tails of the dispersal kernel k are thin

$_{103}$ (i.e., go to zero at least exponentially fast), so that the probability that an individual

$_{104}$ disperses an extremely large distance is exceedingly small.

$_{105}$ In general, both the dispersing fraction p and the dispersal kernel k may depend

$_{106}$ on the population density at the natal location, as does the reproduction function

$_{107}$ f. The way that the functions f, p, and k depend on population density determine

$_{108}$ the dynamics of Eq. 1. In the simplest case, the reproduction function f is strictly

$_{109}$ compensatory; that is, f is an increasing but decelerating function of density $(f'(n) >$

$_{110}$ 0 and $f''(n) < 0)$. For strictly compensatory models, the population will spread at a

$_{111}$ constant asymptotic speed (Fig. 1a) if three conditions hold: small populations grow

$_{112}$ $(f'(0) > 1)$, all individuals disperse $(p = 1)$, and dispersal distance is independent of

$_{113}$ population density. Here, the speed is determined by the growth and spread of the

$_{114}$ low-density populations far ahead of the main invasion front (56); the dynamics at

$_{115}$ high densities do not matter – the hallmark of a pulled invasion.

$_{116}$ Constant asymptotic invasion speeds are not, however, limited to the simple case

5

117 just described. In the absence of Allee effects, they can also occur if the reproduction

118 function produces overcompensation—declining offspring production with increasing

119 population density (so that $f'(1) < 0$). As with classic non-spatial models, over-

120 compensation produces oscillations in population density (26; 5; 48), which in turn

121 cause dynamic changes in the shape of the wave behind the invasion front. Despite

122 these complex fluctuations at high population densities, the invasion speeds of over-

123 compensatory models (without Allee effects) remain constant (Fig. 1b), and are still

124 determined by the dynamics at low densities (19).

125   Long-standing theory suggests that invaders subject to Allee effects at low pop-

126 ulation density and compensatory dynamics at larger population density, will also

127 eventually spread at a constant speed if their initial population sizes are sufficiently

128 large and the Allee effect is not too strong (55; 21). Allee effects cause invasion waves

129 to be pushed from behind their leading edge (16; 55). When Allee effects are suffi-

130 ciently strong, the invasion speed no longer depends upon the pull of populations at

131 low densities in front of the wave, but rather on the strength of the push from the

132 high density populations behind it. In our models, we show that when low-density

133 Allee effects combine with spatiotemporal population density fluctuations (created

134 through overcompensation or density-dependent dispersal), the invasion speed may

135 not be constant asymptotically, as expected under classic invasion theory, but may

136 rather exhibit persistent fluctuations (Fig. 1c-f).

Allee effects and overcompensation

138 First, we investigated whether combining an Allee effect with overcompensation at

139 high population density could induce fluctuating invasion speeds when dispersal is

140 density-independent and all offspring disperse (i.e., $p = 1$). This model (the 'over-

141 compensatory model', see Materials and Methods, Fig. S1a) has two important pa-

142 rameters: r, which affects both the growth rate at low density and the strength of

143 density dependence at carrying capacity, and a, the Allee threshold. We assume that

6

¹⁴⁴ when the population density falls below a, no offspring are produced there (a strong

¹⁴⁵ Allee effect). If the population density falls below a everywhere, the population is

¹⁴⁶ doomed to extinction.

¹⁴⁷ Simulations (described in Materials and Methods) revealed this model generates

¹⁴⁸ variable-speed invasions (Fig. 1c), but only when the low-density Allee threshold is

¹⁴⁹ of intermediate value and high-density overcompensation is strong ($r > 2$, Fig. 2a).

¹⁵⁰ For $r > 2$, the local equilibrium density $n_t(x) = 1$ is unstable, leading to sustained

¹⁵¹ fluctuations in local density. Our simulations suggest $r > 2$ is a necessary condition for

¹⁵² fluctuating invasion speeds in the overcompensatory model. If the Allee threshold (a)

¹⁵³ is too large, the spreading population eventually falls below the threshold everywhere

¹⁵⁴ and is extirpated. If a is sufficiently small, the invasion proceeds with an apparently

¹⁵⁵ constant speed (Fig. 2a).

¹⁵⁶ These fluctuations are induced by the combination of a strong Allee effect, which

¹⁵⁷ produces a pushed wave, and strong overcompensation, which produces large spa-

¹⁵⁸ tiotemporal variation in density behind the invasion front and thus variation in the

¹⁵⁹ strength of the push (Fig. 3). When the population density at any location is smaller

¹⁶⁰ than the Allee threshold (a), as at the leading edge of the wave, the population

¹⁶¹ vanishes before the next time step. Populations just above a become large after re-

¹⁶² production, but as the population size increases beyond a, the offspring population

¹⁶³ size $f(n(x))$ declines as a result of overcompensation (Fig. S1a). Therefore, when

¹⁶⁴ reproduction occurs (transition between $n(x)$ and $f(n(x))$, Fig. 3 black vs blue), pop-

¹⁶⁵ ulations with the highest density become populations of low density, and populations

¹⁶⁶ with density just above a become high density. Through time, this creates variability

¹⁶⁷ in the size of the push by varying the size of the region contributing to the wave

¹⁶⁸ front, leading to fluctuating invasion speeds (Fig. 3d, S3a-f). The speed fluctuations

¹⁶⁹ can be periodic or more complex (Fig. S2). They vary in amplitude by as much as

¹⁷⁰ 100% of the mean speed, with some parameter combinations reaching amplitudes of

171 ∼ 400% of the mean speed (Fig. 2a).

172   This mechanism for variable-speed invasion does not depend on the discreteness

173 of time. We developed a continuous-time version of the overcompensatory model,

174 where we find fluctuating invasion speeds as long as density fluctuations behind the

175 wave front combine with strong low-density Allee effects (SI Appendix, Fig. S4-6).

Allee effects and density-dependent dispersal

177 Overcompensation is not the only mechanism that can generate the spatiotemporal

178 variability in population density that is necessary to produce fluctuating invasion

179 speeds when combined with Allee effects. Density-dependent dispersal, manifest as

180 either density-dependence in the propensity to disperse (p) or in the shape of the

181 dispersal-kernel (k), can generate this high-density variability in the pushing force

182 as well. We demonstrate this result with two models (the 'propensity model' and

183 the 'distance model', respectively, see Materials and Methods), both built upon a

184 piecewise linear growth function that is compensatory at high population density

185 (Fig. S1b). We continue to include low-density Allee effects. When the population

186 size falls below the threshold density a, individuals produce offspring at the constant

187 per capita rate λ. Alternatively, if the population size exceeds a, the population goes

188 to carrying capacity.

189   In the propensity model, population density influences the propensity to disperse

190 (p). In particular, we assume that the proportion of offspring that disperse is given

191 by a logistic function of local population density ($n_t(x)$) (Eq. 5) with four parameters:

192 the minimum (p_0) and maximum ($p_{\max}$) dispersal proportion; a location parameter

193 $\hat{n}$, which is the density at which the dispersal propensity is halfway between p_0 and

194 $p_{\max}$; and a shape parameter α. The sign of α determines if the proportion dispersing

195 increases ($\alpha > 0$) or decreases ($\alpha < 0$) with density (Fig. S1c). The larger the

196 magnitude of α the steeper the density response, which is centered around $\hat{n}$.

197   The propensity model can also generate invasions that spread at fluctuating speeds

8

198 (Fig. 1d, S7). We found these fluctuations persist only when Allee effects are strong

199 $(0 \leq \lambda < 1)$, dispersal propensity increases with population density $(\alpha > 0)$, and

200 the dispersal response occurs at a population density that is larger than the Allee

201 threshold $(\hat{n} > a)$. Fluctuations in speed are nearly always periodic (Fig. S7c, S8a-

202 d) and of large amplitude, altering the invasion speed by $\sim 100\% - 750\%$ relative to

203 the mean speed (Fig. 2b). These large-amplitude periodic fluctuations often include

204 positive and negative speeds, meaning that invasions alternate between steps forward

205 and smaller steps backward (Fig. 1d).

206 As before, spreading speed fluctuations are created through variations in the dis-

207 persing population that pushes the invasion forward from behind the front (Fig. 1d).

208 The magnitude of the push depends on the width of the region contributing dispersing

209 individuals, and the proximity of this region to the front (Fig. S3g-l). When density

210 dependence in dispersal is strong and positive (large α), the population directly ad-

211 jacent to the front is below the Allee effect threshold (a) and therefore decays to zero

212 (Fig. S3g-h). Farther behind the front, density is above a, but below the dispersal

213 midpoint $(\hat{n})$, thus this region of the population reproduces but does not disperse

214 (Fig. S3h-i). This action results in a large push from behind the wave front that

215 moves the invasion forward at the next time step when the non-dispersing popula-

216 tion eventually disperses (Fig. S3i-k). Subsequently, the region of the non-dispersing

217 population is much smaller and farther from the invasion front at the next time step,

218 resulting in a much smaller push (Fig. S3k).

219 With the distance model we explore a second type of density-dependent dispersal,

220 where density alters the dispersal distance. Here, all offspring disperse $(p = 1)$, but

221 density alters the variance (σ^2) of the dispersal kernel (Eq. 6). Four parameters

222 control this dependence: σ_0^2 and $\sigma_{\max}^2$, which are the lower and upper bounds of the

223 variance; the location parameter, $\hat{n}$ which is the density at which dispersal variance

224 is halfway between σ_0^2 and $\sigma_{\max}^2$; and a shape parameter β. The dispersal variance

9

225 increases with population density when β is positive, and decreases with density when

226 β is negative. The larger the absolute value of β, the sharper the response (Fig S1d).

227 The distance model also produces the necessary spatiotemporal variability in

228 population density behind the invasion front to induce fluctuating invasion speeds

229 (Fig. 1e,f, S7). As in the propensity model, the invasion speed only fluctuates when

230 Allee effects are strong ($0 \leq \lambda \leq 1$). However, unlike the propensity model, we find

231 persistent fluctuations are possible when density-dependent dispersal is both positive

232 ($\beta > 0$) and negative ($\beta < 0$) (Fig. 2c). The speed fluctuations are more frequently

233 aperiodic (Fig. S8e-h) than the two-cycle fluctuations seen in the propensity model,

234 with largest amplitude when dispersal distance increases with density ($\beta > 0$) (Fig. 2c,

235 S7f). In general, fluctuations are larger as both Allee effects and density-dependent

236 dispersal are stronger, and alter the invasion speed by $\sim 5\% - 100\%$ ($\beta > 0$), and

237 $\sim 1\% - 9\%$ ($\beta < 0$) relative to the mean speed (Fig. 2c, S7f).

238 When the dispersal distance exhibits strong positive density dependence (Fig. S3m-

239 r), populations at densities above the dispersal threshold disperse long distances, and

240 those below disperse short distances. In this model, each push forward is made up

241 of a combination of both short and long distance dispersers. The size of this push

242 changes depending on the proportion of the push made up of each type of disperser,

243 which is temporally variable, creating fluctuating invasion speeds. A similar mech-

244 anism operates when $\beta < 0$ (Fig. S3s-x), however instead high density populations

245 disperse short distances and vice versa.

Discussion

247 Our work provides novel insight into mechanisms behind invasion variability: fluc-

248 tuations in invasion speed can occur solely due to endogenous density dependence.

249 In the models we examine, both a strong low-density Allee effect (creating a pushed

250 wave (9; 28)), and large variations in population density behind the invasion front

10

251 are necessary to create fluctuating invasion speeds. We demonstrate that the neces-
252 sary spatiotemporal variability can be generated via two types of density feedbacks:
253 overcompensatory density dependence, or density-dependent dispersal. When com-
254 bined with Allee effects, either of these factors can cause the strength of the invasion
255 push from high density populations to vary, leading to varying spreading speeds.
256 The potential for deterministic, density-dependent processes to generate complex
257 fluctuations in local population density is a canonical result of theoretical popula-
258 tion biology (15; 26; 5; 48) and has proven influential in basic and applied empirical
259 settings (36). By considering the spatial dimension of population growth, which is
260 increasingly relevant in the context of global change, our new results flesh out under-
261 standing of complex population dynamics arising from endogenous mechanisms. We
262 conjecture that there is some generality to this mechanism as we also see fluctuating
263 speeds in continuous time (SI Appendix, Fig. S4), although we recognize fluctuations
264 can occur through other means (e.g. (7; 33; 14)). Our results are potentially con-
265 sistent with the highly variable spreading speeds seen in empirical invasion studies
266 (14; 34; 59; 54; 4; 60).

267 Processes capable of generating fluctuations in population density that create the
268 variable pushing force behind the invasion vanguard are common in nature. First,
269 many invasive species show the combination of high intrinsic growth rates and con-
270 specific interference at high density that gives rise to overcompensatory population
271 fluctuations (36; 61). Second, density dependent dispersal as a distinct source of
272 spatiotemporal density fluctuations can arise even with strictly compensatory den-
273 sity dependence in population growth. We found fluctuating invasion speeds with
274 positive density-dependent dispersal propensity, which is common in organisms with
275 environmentally inducible dispersal polymorphisms, including many insects. For ex-
276 ample, wingless aphids (11; 13) and planthoppers (38) can produce winged morphs
277 when densities become high. When density dependence alters dispersal distance,

11

₂₇₈ fluctuations in speed were seen under both positive and negative density dependence.
₂₇₉ Mobile organisms can increase their dispersal distance with increasing density by al-
₂₈₀ tering behavioral responses (25). Alternatively, dispersal distances can decrease with
₂₈₁ density when crowding decreases reproductive and dispersal ability (24; 6; 25), or in
₂₈₂ animals (notably small mammals) with strong group behavior (12; 2; 25).

₂₈₃   Allee effects, a common density-dependent process (18; 31), influence small pop-
₂₈₄ ulations by decreasing low-density vital rates (e.g., reproduction (51)). We find in
₂₈₅ all of our models that Allee effects, and the pushed invasions that they generate,
₂₈₆ are a necessary ingredient of fluctuating speeds. Interestingly, this result contrasts
₂₈₇ with Dwyer and Morris (7). Working with a two-species model, they found that fluc-
₂₈₈ tuating speeds can occur when predator dispersal distance depends on prey density
₂₈₉ (a type of density dependent movement) but without an explicit Allee effect. We
₂₉₀ conjecture that predator-prey dynamics in their model may in fact give rise to an
₂₉₁ implicit Allee effect, as is known to occur in other predator-prey models (33). Bio-
₂₉₂ logically, density-dependent movement can contribute to an Allee effect by reducing
₂₉₃ mate finding abilities at low densities, especially when the movement is sex biased
₂₉₄ (53; 41). In this way, the study by Dwyer and Morris (7), while superficially incon-
₂₉₅ sistent with ours, may nonetheless satisfy the conditions we identify as necessary for
₂₉₆ variable invasions.

₂₉₇   Thoroughly accounting for the sources of variability in the speed of biological
₂₉₈ invasions may improve invasion forcasting. Our work suggests that intrinsic density
₂₉₉ dependence can create complex invasion dynamics, consistent with the highly variable
₃₀₀ spreading speeds seen in empirical invasion studies (34; 59; 60; 14; 4; 54). However,
₃₀₁ it remains an open question whether and how often these processes affect the ecologi-
₃₀₂ cal dynamics of spread, given the pervasive influences of environmental heterogeneity
₃₀₃ (43; 33; 57; 58; 3; 40) and demographic stochasticity (35; 17; 42), and their roles in
₃₀₄ invasion variability. To begin to answer this question, we suggest coupling models

305 and empirical data, which has proven to be a fruitful approach to understanding the

306 intrinsic mechanisms behind fluctuations in local population density (e.g., (5; 48)).

307 Collecting long-term data can be difficult, but some patterns might be straightforward

308 to identify from existing datasets. In particular, the strong two-cycle speed fluctu-

309 ations generated when invaders experience both Allee effects and density-dependent

310 dispersal propensity would likely be detectable in data. Few empirical studies have

311 tested for endogenous mechanisms of fluctuating invasion speeds, including studies

312 for which variability in speed was an explicit focus (53; 27; 29; 34; 59) (but see (14)).

313 Thus, signatures of endogenous variability may be embedded in existing data, and

314 we encourage empiricists to re-examine variable invasion data in the context of these

315 density-dependent mechanisms.

Materials and Methods

317 The models we studied are each a special case of equation (1). They all use the

318 Laplace dispersal kernel with variance σ^2:

$$k(x - y; \sigma^2) = \frac{1}{\sqrt{2\sigma^2}} \exp\left[-\sqrt{\frac{2(x - y)^2}{\sigma^2}}\right]. \tag{2}$$

319 Qualitative results are robust to kernel choice (i.e. Normal, Cauchy).

Overcompensatory Model

321 We combine low-density Allee effects with the possibility of overcompensation at high

322 density (Fig. S1a):

$$f(n) = \begin{cases} n \exp\Big(r(1 - n)\Big) & \text{for } n > a, \\ \\ 0 & \text{for } n \leq a. \end{cases} \tag{3}$$

13

323 Dispersal is independent of density in this model ($\sigma^2(n) = \sigma^2$, a constant) and all

324 offspring disperse ($p = 1$).

Propensity Model

326 Here, we used a linear-constant model for growth

$$
f(n) = \begin{cases} \lambda n & \text{for } n < a \\ \\ 1 & \text{for } n \geq a, \end{cases} \tag{4}
$$

327 where $0 \leq a < 1$ (Fig. S1b). Dispersal propensity depends upon the population

328 density ($n_t(x)$) via a logistic form similar to other models with density-dependent

329 dispersal (Fig. S1c) (45):

$$
p(n) = p_0 + \left\{ \frac{p_{max} - p_0}{1 + \exp\left[-\alpha\left(n - \hat{n}\right)\right]} \right\}. \tag{5}
$$

330 As in the overcompensatory model, the distance moved by dispersing individuals is

331 independent of density ($\sigma^2(n) = \sigma^2$, a constant).

Distance Model

333 For this model, we use the reproduction function (4), but assume all offspring disperse

334 ($p = 1$) following a dispersal distribution whose variance is a logistic function of

335 parental density ($n_t(x)$) (Fig. S1d). I.e.,

$$
\sigma^2(n) = \sigma_0^2 + \left\{ \frac{\sigma_{max}^2 - \sigma_0^2}{1 + \exp\left[-\beta\left(n - \hat{n}\right)\right]} \right\}. \tag{6}
$$

336 We simulated each model for 200 iterations across a domain of length 1200 with

337 $2^{16} + 1$ spatial nodes. Within each simulation, we defined the location of the invasion

338 front at each time step as the location where the density of the invasion wave first

339 exceeded a density threshold of 0.05. We then used this location to calculate: (1)

14

340 the instantaneous invasion speed (i.e., the distance traveled by the front between

341 consecutive time steps), (2) the mean invasion speed averaged over the last 50 time

342 steps, and (3) the amplitude of invasion speed fluctuations (the difference between

343 the maximum and minimum speed over the last 20 time steps). See Table S1 for a

344 list of parameters and definitions. Code to run these models and recreate all figure

345 will be available at Dryad upon manuscript acceptance.

Acknowledgements

15

References

[1] Andow, D. A., Kareiva, P. M., Levin, S. A., and Okubo, A. (1990). Spread of invading organisms. *Landsc Ecol*, 4(2-3):177–188.

[2] Andreassen, H. P. and Ims, R. A. (2001). Dispersal in patchy vole populations: Role of patch configuration, density dependence, and demography. *Ecol*, 82(10):2911–2926.

[3] Caswell, H., Neubert, M. G., and Hunter, C. M. (2011). Demography and dispersal: invasion speeds and sensitivity analysis in periodic and stochastic environments. *Theor Ecol*, 4(4):407–421.

[4] Chen, H. (2014). A spatiotemporal pattern analysis of historical mountain pine beetle outbreaks in British Columbia, Canada. *Ecography*, 37(4):344–356.

[5] Costantino, R. F., Desharnais, R. A., Cushing, J. M., and Dennis, B. (1997). Chaotic dynamics in an insect population. *Science*, 275(5298):389–391.

[6] Donohue, K. (1998). Maternal determinants of seed dispersal in Cakile edentula: Fruit, plant, and site traits. *Ecol*, 79(8):2771–2788.

[7] Dwyer, G. and Morris, W. F. (2006). Resource-dependent dispersal and the speed of biological invasions. *Am Nat*, 167(2):165–76.

[8] Fagan, W. F., Lewis, M. A., Neubert, M. G., and van den Driessche, P. (2002). Invasion theory and biological control. *Ecol Lett*, 5(1):148–157.

[9] Gandhi, S. R., Yurtsev, E. A., Korolev, K. S., and Gore, J. (2016). Range expansions transition from pulled to pushed waves as growth becomes more cooperative in an experimental microbial population. *Proc Natl Acad Sci USA*, 113(25):6922–6927.

[10] Gurney, W. S. C., Blythe, S. P., and Nisbet, R. M. (1980). Nicholson's blowflies revisited. *Nature*, 287:17–21.

[11] Harrison, R. G. (1980). Dispersal polymorphisms in insects. *Annu Rev Ecol Syst*, 11:95–118.

[12] Ims, R. A. and Andreassen, H. P. (2005). Density-dependent dispersal and spatial population dynamics. *Proc Roy Soc B*, 272(1566):913–918.

[13] Johnson, B. (1965). Wing polymorphism in aphids II. Interactions between aphids. *Entomologia Experimentalis et Applicata*, 8(1):49–64.

[14] Johnson, D. M., Liebhold, A. M., Tobin, P. C., and Bjørnstad, O. N. (2006). Allee effects and pulsed invasion by the gypsy moth. *Nature*, 444(7117):361–363.

[15] Kingsland, S. E. (1995). *Modeling nature*. University of Chicago Press.

[16] Kot, M., Lewis, M. A., and van den Driessche, P. (1996). Dispersal data and the spread of invading organisms. *Ecol*, 77(7):2027–2042.

[17] Kot, M., Medlock, J., Reluga, T., and Walton, D. B. (2004). Stochasticity, invasions, and branching random walks. *Theor Popul Biol*, 66(3):175–184.

[18] Kramer, A. M., Dennis, B., Liebhold, A. M., and Drake, J. M. (2009). The evidence for Allee effects. *Pop Ecol*, 51(3):341–354.

[19] Li, B., Lewis, M. A., and Weinberger, H. F. (2009). Existence of traveling waves for integral recursions with nonmonotone growth functions. *J Math Biol*, 58(3):323–338.

[20] Lin, C., Lin, C., Lin, Y., and Mei, M. (2014). Exponential stability of non-monotone traveling waves for Nicholson's blowflies equation. *SIAM J Math Anal*, 46(2):1053–1084.

17

[21] Lui, R. (1983). Existence and stability of travelling wave solutions of a nonlinear integral operator. *J Math Biol*, 16(3):199–220.

[22] Lutscher, F. (2008). Density-dependent dispersal in integrodifference equations. *J Math Biol*, 56(4):499–524.

[23] Lutscher, F. and Van Minh, N. (2013). Traveling waves in discrete models of biological populations with sessile stages. *Nonlinear Anal: Real World Appl*, 14(1):495–506.

[24] Marchetto, K. M., Jongejans, E., Shea, K., and Isard, S. A. (2010). Plant spatial arrangement affects projected invasion speeds of two invasive thistles. *Oikos*, 119(9):1462–1468.

[25] Matthysen, E. (2005). Density-dependent dipsersal in birds and mammals. *Ecography*, 28(3):403–416.

[26] May, R. M. (1974). Biological populations with nonoverlapping generations: Stable points, stable cycles, and chaos. *Science*, 186(4164):645–647.

[27] Melbourne, B. A. and Hastings, A. (2009). Highly variable spread rates in replicated biological invasions: Fundamental limits to predictability. *Science*, 325:1536–1539.

[28] Mendez, V., Llopis, I., Campos, D., and Horsthemke, W. (2011). Effect of environmental fluctuations on invasion fronts. *J Theor Biol*, 281(1):31–38.

[29] Miller, T. E. X. and Inouye, B. D. (2013). Sex and stochasticity affect range expansion of experimental invasions. *Ecol Lett*, 16:354–361.

[30] Miller, T. E. X. and Tenhumberg, B. (2010). Contributions of demography and dispersal parameters to the spatial spread of a stage-structured insect invasion. *Ecol Appl*, 20(3):620–633.

18

[31] Morris, D. W. (2002). Measuring the Allee effect: Positive density dependence in small mammals. *Ecol*, 83(1):14–20.

[32] Neubert, M. G. and Caswell, H. (2000). Demography and dispersal: Calculation and sensitivity analysis of invasion speed for structured populations. *Ecol*, 81(6):1613–1628.

[33] Neubert, M. G., Kot, M., and Lewis, M. A. (2000). Invasion speeds in fluctuating environments. *Proc Roy Soc B*, 267:1603–1610.

[34] Ochocki, B. M. and Miller, T. E. X. (2017). Rapid evolution of dispersal ability makes biological invasions faster and more variable. *Nat Commun*, 8:14315.

[35] Pachepsky, E. and Levine, J. M. (2011). Density dependence slows invader spread in fragmented landscapes. *Am Nat*, 177(1):18–28.

[36] Pardini, E. A., Drake, J. M., Chase, J. M., and Knight, T. M. (2009). Complex population dynamics and control of the invasive biennial Alliaria petiolata (garlic mustard). *Ecol Appl*, 19(2):387–397.

[37] Peltonen, M., Liebhold, A. M., Bjørnstad, O. N., and Williams, D. W. (2002). Spatial synchrony in forest insect outbreaks: Roles of regional stochasticity and dispersal. *Ecol*, 83(11):3120–3129.

[38] Robert F. Denno, G. K. R. (1992). Density-related dispersal in planthoppers: Effects of interspecific crowding. *Ecol*, 73(4):1323–1334.

[39] Sakai, A. K., Allendorf, F. W., Holt, J. S., Lodge, D. M., Molofsky, J., With, K. A., Baughman, S., Cabin, R. J., Cohen, J. E., Ellstrand, N. C., McCauley, D. E., O'Neil, P., Parker, I. M., Thompson, J. N., and Weller, S. G. (2001). The population biology of invasive species. *Annu Rev Ecol Syst*, 32:305–332.

[40] Schreiber, S. J. and Ryan, M. E. (2011). Invasion speeds for structured populations in fluctuating environments. *Theor Ecol*, 4(4):423–434.

[41] Shaw, A. K., Kokko, H., and Neubert, M. G. (in press). Sex differences and Allee effects shape the dynamics of sex-structured invasions. *J Anim Ecol*.

[42] Shen, W. (2004). Traveling waves in diffusive random media. *J Dyn Diff Equ*, 16(4):1011–1060.

[43] Shigesada, N., Kawasaki, K., and Teramoto, E. (1986). Traveling periodic waves in hetergeneous environments. *Theor Popul Biol*, 30:143–160.

[44] Skellam, J. G. (1951). Random dispersal in theoretical populations. *Biometrika*, 38(1):196–218.

[45] Smith, M. J., Sherratt, J. A., and Lambin, X. (2008). The effects of density-dependent dispersal on the spatiotemporal dynamics of cyclic populations. *J Theor Biol*, 254(2):264–274.

[46] Solar, A. and Trofimchuk, S. (2015). Asymptotic convergence to pushed wavefronts in a monostable equation with delayed reaction. *Nonlinearity*, 28(7):2027–2052.

[47] Taylor, C. M. and Hastings, A. (2005). Allee effects in biological invasions. *Ecol Lett*, 8:895–908.

[48] Turchin, P. (2003). *Complex population dynamics: A theoretical/empirical synthesis*. Princeton University Press.

[49] van den Bosch, F., Hengeveld, R., and Metz, J. A. J. (1992). Analysing the velocity of animal range expansion. *J of Biogeogr*, 19(2):135–150.

[50] van Saarloos, W. (2003). Front propagation into unstable states. *Physics Reports*, 386:29–222.

[51] Veit, R. R. and Lewis, M. A. (1996). Dispersal, population growth, and the Allee Effect: Dynamics of the house finch invasion of eastern North America. *Am Nat*, 148(2):255–274.

[52] Volkov, D. and Lui, R. (2007). Spreading speed and travelling wave solutions of a partially sedentary population. *IMA J Appl Math*, 72(6):801–816.

[53] Wagner, N. K., Ochocki, B. M., Crawford, K. M., Compagnoni, A., and Miller, T. E. (2016). Genetic mixture of multiple source populations accelerates invasive range expansion. *J Anim Ecol*, 86(1):21–34.

[54] Walter, J. A., Johnson, D. M., Tobin, P. C., and Haynes, K. J. (2015). Population cycles produce periodic range boundary pulses. *Ecography*, 38:1200–1211.

[55] Wang, M.-H., Kot, M., and Neubert, M. G. (2002). Integrodifference equations, Allee effects, and invasions. *J Math Biol*, 44:150–168.

[56] Weinberger, H. F. (1982). Long-time beahvior of a class of biological models. *SIAM J Math Anal*, 13(3):353–396.

[57] Weinberger, H. F. (2002). On spreading speeds and traveling waves for growth and migration models in a periodic habitat. *J Math Biol*, 45(6):511–548.

[58] Weinberger, H. F., Kawasaki, K., and Shigesada, N. (2008). Spreading speeds of spatially periodic integrodifference models for populations with nonmonotone recruitment functions. *J Math Biol*, 57(3):387–411.

[59] Weiss-Lehman, C., Hufbauer, R. A., and Melbourne, B. A. (2017). Rapid trait evolution drives increased speed and variance in experimental range expansions. *Nat Commun*, 8:14303.

[60] Williams, J. L., Kendall, B. E., and Levine, J. M. (2016). Rapid evolution accelerates plant population spread in fragmented experimental landscapes. *Science*, 353:482–485.

[61] Zipkin, E. F., Kraft, C. E., Cooch, E. G., and Sullivan, P. J. (2009). When can efforts to control nuisance and invasive species backfire? *Ecol Appl*, 19(6):1585–1595.

501   # Figures

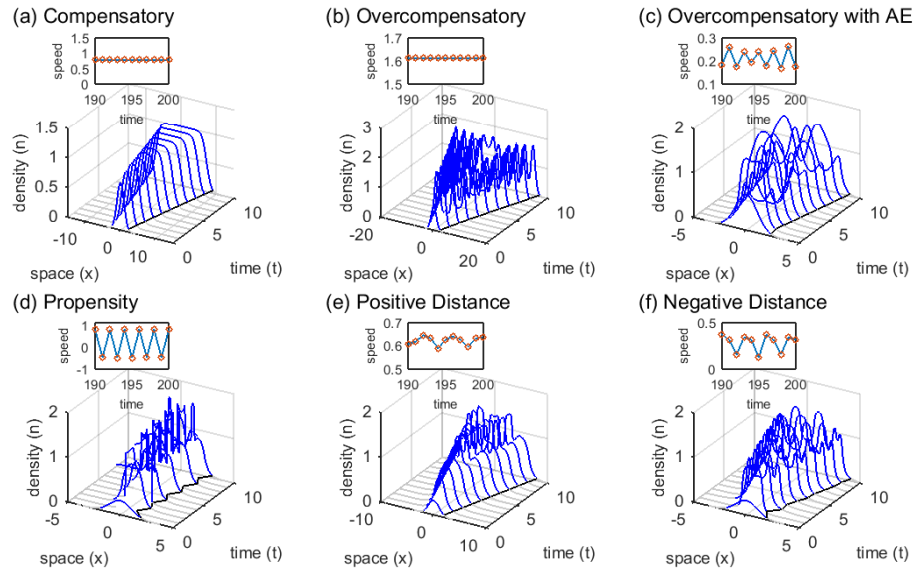Figure 1: Invasion dynamics under different types of density dependence and dispersal. With compensatory growth at high densities (a), the wave shape and invasion speed are both constant. This is true with and without low-density Allee effects (overcompensatory model: $\sigma^2 = 0.25$, $a = 0$, and $r = 0.9$; Fig. S1a). With overcompensatory population growth and no Allee effect (b), population density exhibits fluctuations behind the front yet the leading edge progresses at a constant speed (overcompensatory model: $\sigma^2 = 0.25$, $a = 0$, and $r = 2.7$; Fig. S1a). However, when overcompenstion combines with low-density Allee effects (c), the invasion speed fluctuates (overcompensatory model: $\sigma^2 = 0.25$, $a = 0.4$, and $r = 2.7$; Fig. S1a). Variability in invasion speed can also occur when Allee effects combine with density-dependence in the proportion of dispersing offspring (d) (propensity model: $a = 0.2$, $\lambda = 0$, $\hat{n} = 0.9$, $p_0 = 0.05$, $p_{max} = 1$, $\alpha = 50$), or in dispersal distance (e,f). In the latter model, dispersal distance decreases with population density (e) (distance model: $a = 0.2$, $\lambda = 0$, $\hat{n} = 0.9$, $\beta = -50$, $\sigma_0^2 = 0.05$, $\sigma_{max}^2 = 1$), or increases with density (f) (distance model: parameters as in (e) except $\beta = 50$). Initial population densities are either 2 (a-c) or 0.8 (d-f) times the standard normal probability density truncated at $|x| = 5$.
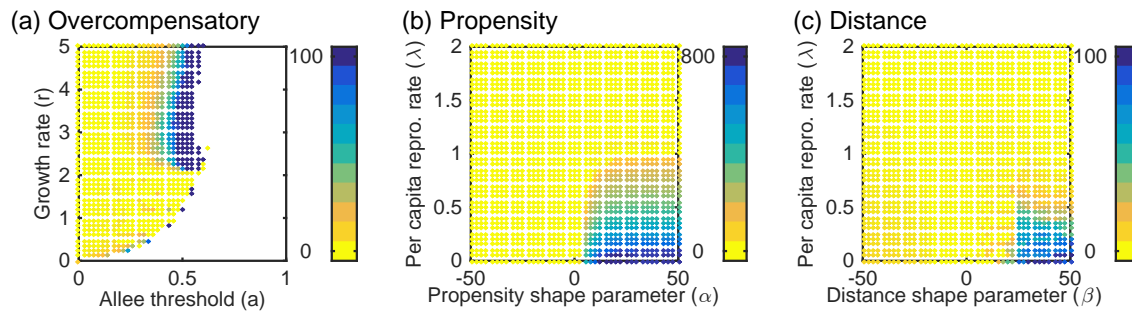
24

Figure 2: Amplitude of fluctuations in invasion speed normalized by the mean speed for populations with Allee effects and (a) overcompensatory growth, (b) density-dependent dispersal propensity, and (c) density-dependent dispersal distance. Darker colors (blue) indicate where fluctuations create large differences from the mean invasion speed. Values of zero (yellow) indicate invasion waves that move at a constant speed. White regions indicate where invasions fail. Parameter values: $\sigma^2 = 0.25$ (a-b); $a = 0.2$, $\hat{n} = 0.9$ (b-c); $p_0 = 0.05$, $p_{max} = 1$ (b); $\sigma_0^2 = 0.05$, $\sigma_{max}^2 = 1$ (c); Initial population densities are equivalent to those in Fig. 1.
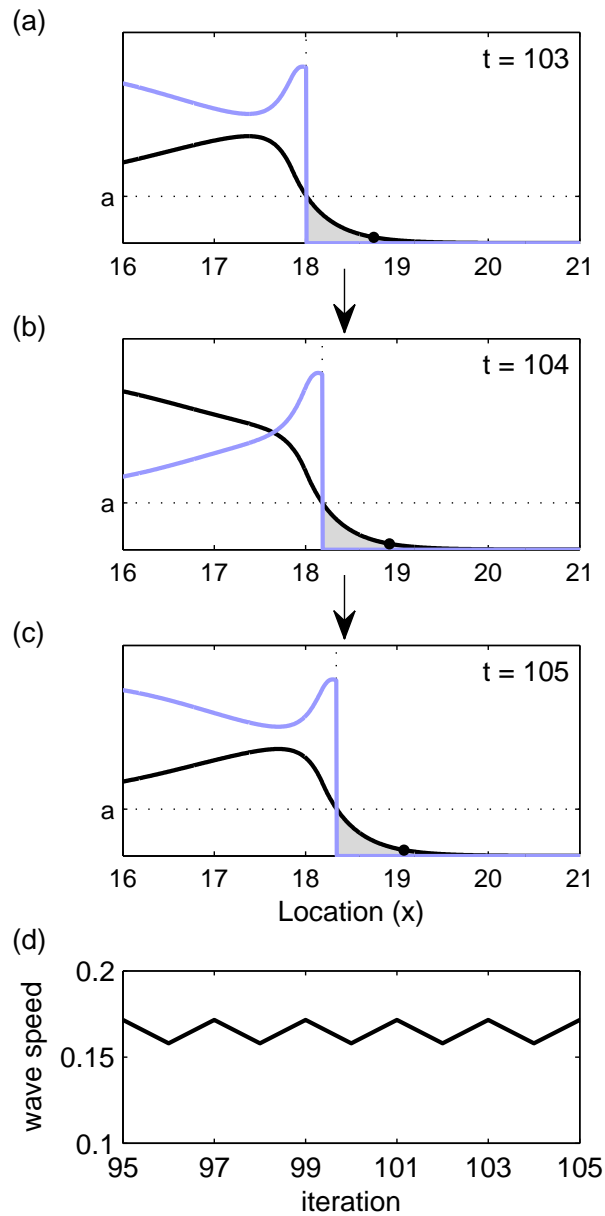
Figure 3: Population density before ($n(x)$ - black curve) and after ($f(n(x))$ - blue curve) growth (overcompensatory model with Allee effects, Eq. 3) at sequential time steps (a-c). Gray regions represent locations that go extinct due to Allee effects (light gray; $n(x) < a$), and the solid point shows the edge of the wave. The wave speed over time (d), corresponds to (a-c). Parameter values include $r = 2.2, a = 0.4, \sigma^2 = 0.25$.

Supporting Information (SI)

502

SI Table

503

504

505

Table 1: All model parameters, definitions and corresponding models.

| Variable	Meaning
t	time
x, y	locations
$n_t(x)$	population density at location x and time t
Parameter	**Meaning**
a	Allee effect threshold
r	intrinsic growth rate (overcompensatory model)
λ	low-density per capita reproductive rate (propensity and distance models)
$\hat{n}$	dispersal density midpoint parameter (propensity and distance models)
p	fraction of offspring that disperse
p_0	minimum dispersal propensity (propensity model)
p_{max}	maximum dispersal propensity (propensity model)
α	propensity shape parameter (propensity model)
σ^2	variance of the dispersal kernel
σ_0^2	minimum dispersal variance (distance model)
σ_{max}^2	maximum dispersal variance (distance model)
β	distance shape parameter (distance model)
Function	**Meaning**
$k(x - y)$	dispersal kernel
$f(n_t(x))$	growth or offspring density

SI Figures

506

507

508

27
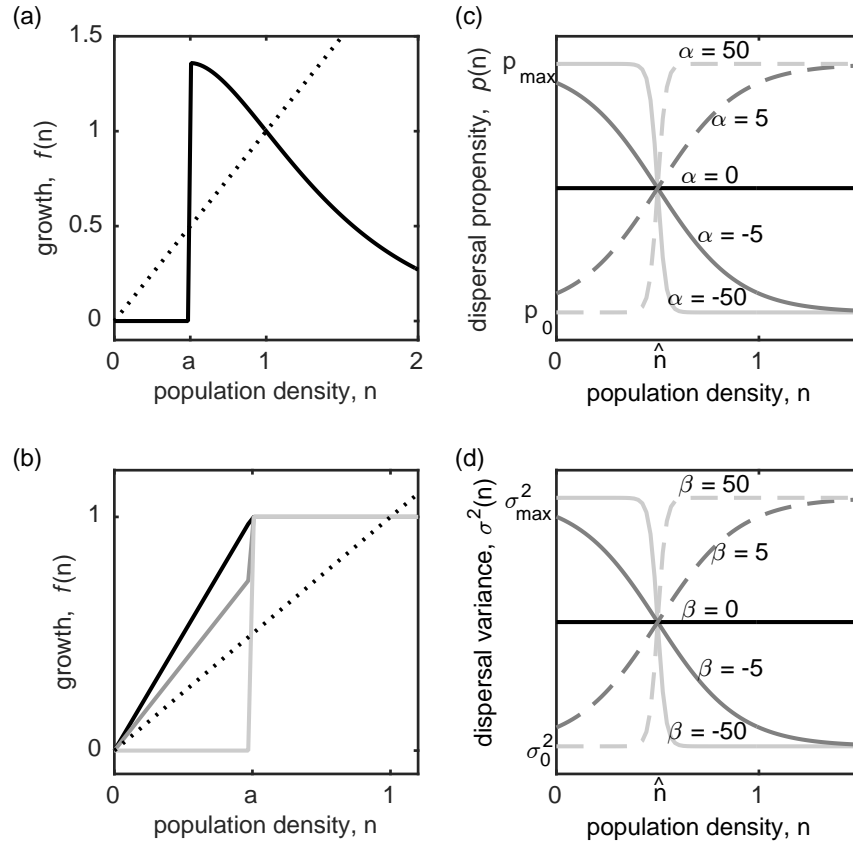
Figure S1: Reproduction and dispersal functions used in the overcompensatory, propensity, and distance models (described in Materials and Methods). (a) The reproductive rate f(n) as given by Eq. 3 where $r = 0.9$ and $a = 0$ (same parameterization as Eq. 3 for Fig 1a, black), $r = 2.7$ and $a = 0$ (same parameterization as Eq. 3 for Fig 1b, dark gray solid), $r = 2.7$ and $a = 0.4$ (same parameterization as Eq. 3 for Fig 1c, light gray dashed). (b) The reproductive rate f(n) as given by Eq. 4 when $a = 0.5$ and $\lambda = 0$ (light gray), $\lambda = 1.5$ (dark gray), $\lambda = 2$ (black). Parameterization here is close to that of Fig 1d-f, except a is smaller here to more clearly visually demonstrate the differences between strong, weak and no Allee effects. (c) The propensity to disperse when altered by density dependence as given by Eq. 5 for different α. (d) The variance of the dispersal kernel when altered by density dependence Eq. 6 for different β values.
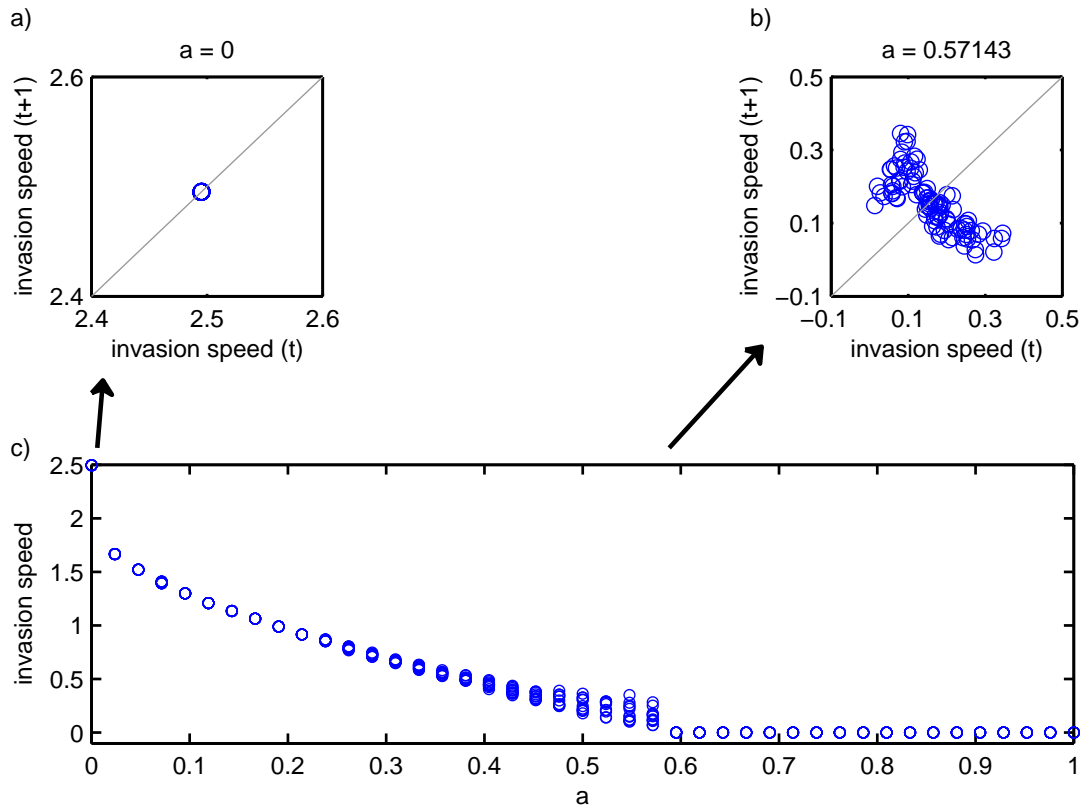
Figure S2: The periodicity of the invasion speed through time for the overcompensatory model - Allee effects and overcompensation. In panels a-b, the wave position is plotted at time t vs time $t+1$. The wave speed ranges in periodicity across values of the Allee effect threshold a. At small values of a the invasion speed is constant (a), and at larger a values (b), the wave speed becomes chaotic until a becomes so large the population goes extinct. In panel (c), the range of invasion speeds represents the amplitude of fluctuations. At each plotted a value, the invasion speed for the previous 100 time steps are plotted. When points appear as hollow points, the same invasion speed is being plotted over itself many times. Here, $\sigma^2 = 0.25$.
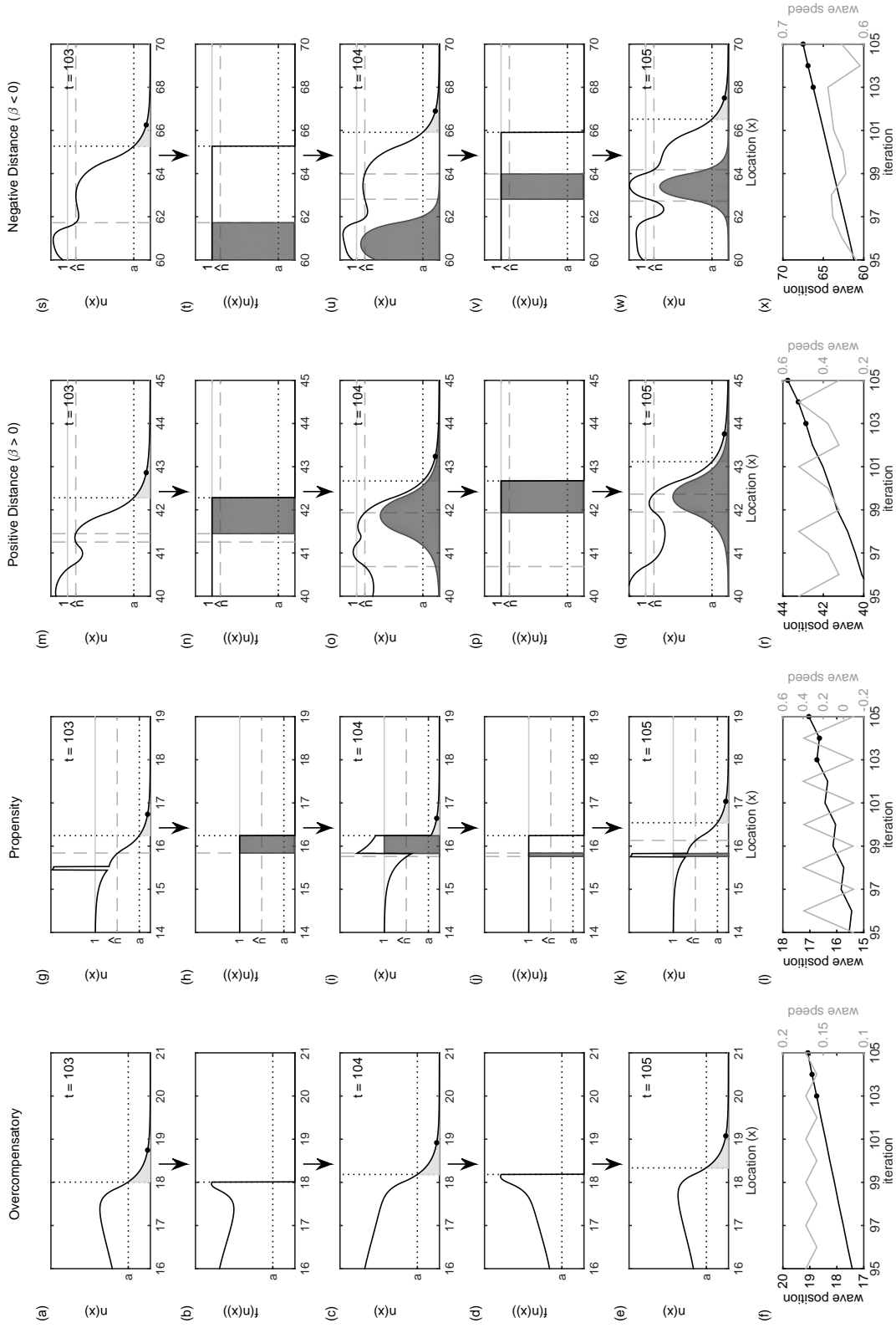
Figure S3: Four examples of fluctuations in invasion speed. The top five rows show the population density before $(n(x))$ and after $(f(n(x)))$ growth at sequential time steps, showing individuals that will not reproduce (light gray; $n < a$), those that do not disperse far (dark gray; $n > \hat{n}$ or $n < \hat{n}$), and the edge of the wave (solid point). The bottom row shows the wave position and speed over time. Parameter values and initial densities are the same as Fig. 2 except: (a-f) $r = 2.2$, $a = 0.4$, (g-l) $\hat{n} = 0.6$, $\alpha \to \infty$, (m-r) $\beta \to \infty$, (s-x) $\beta \to -\infty$.
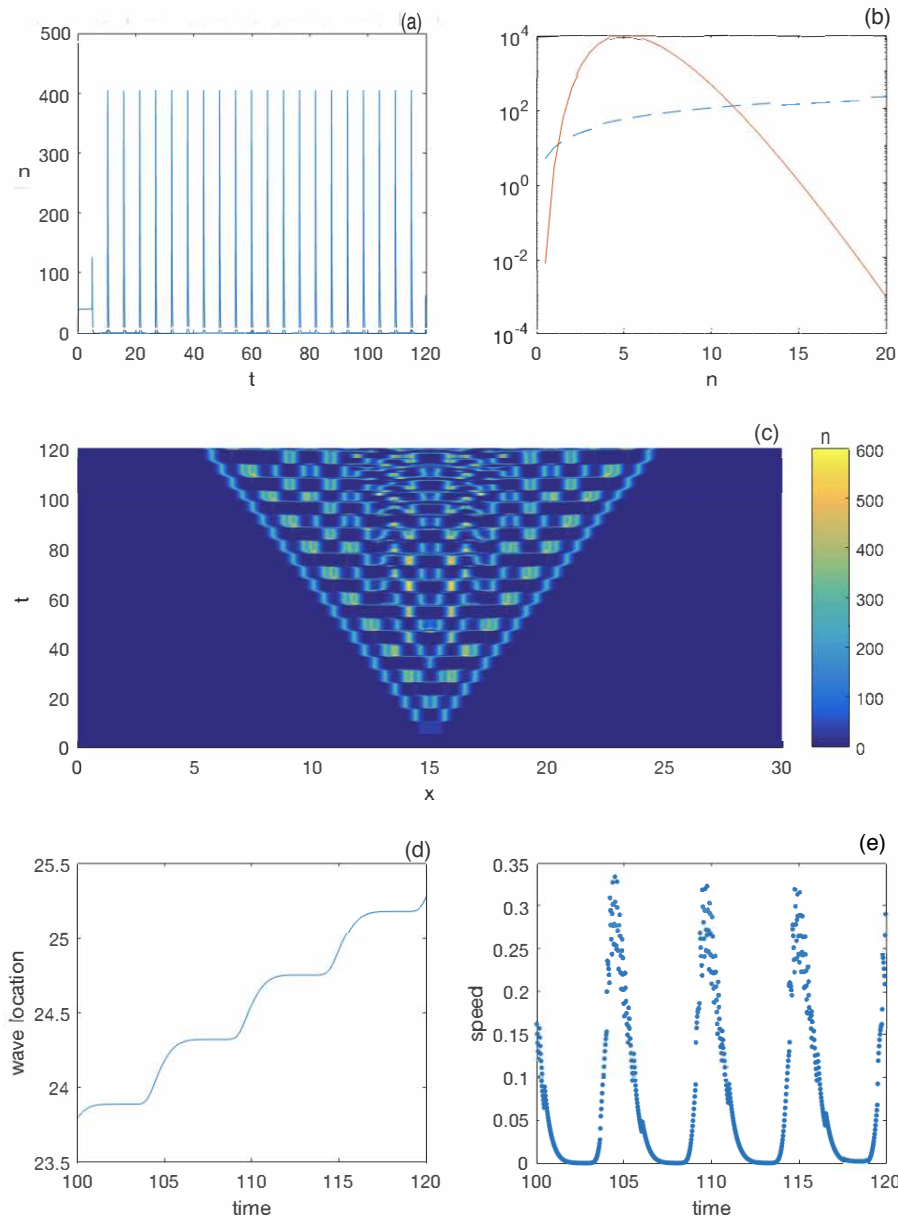
Figure S4: Simulation of model (Eq. 2 from SI Appendix), with $a_1 = 20$, $a_2 = 2$, $a_3 = 10$, $\mu = 10$, $\tau = 5$, and $D = 0.1$. For these parameters the *undelayed* ordinary differential equation (Eq. 2 from SI Appendix with $D = 0$ and $\tau = 0$) exhibits a strong Allee effect, evident by comparing the mortality rate (dashed blue line) to the reproduction rate (solid red curve) in panel (b) (note the logarithmic scale). With delays, the model without movement (Eq. 2 from SI Appendix with $D = 0$) exhibits sharp generational cycles (a). The simulation of the partial functional differential equation (Eq. 2 from SI Appendix; initialized with $n = 2$ for $|x - 15| \leq 0.5$ and $0 \leq t \leq \tau$, and $n = 0$ otherwise) exhibits complex dynamics behind the invading fronts (c). These oscillations push the wave forward with a variable speed (d,e).
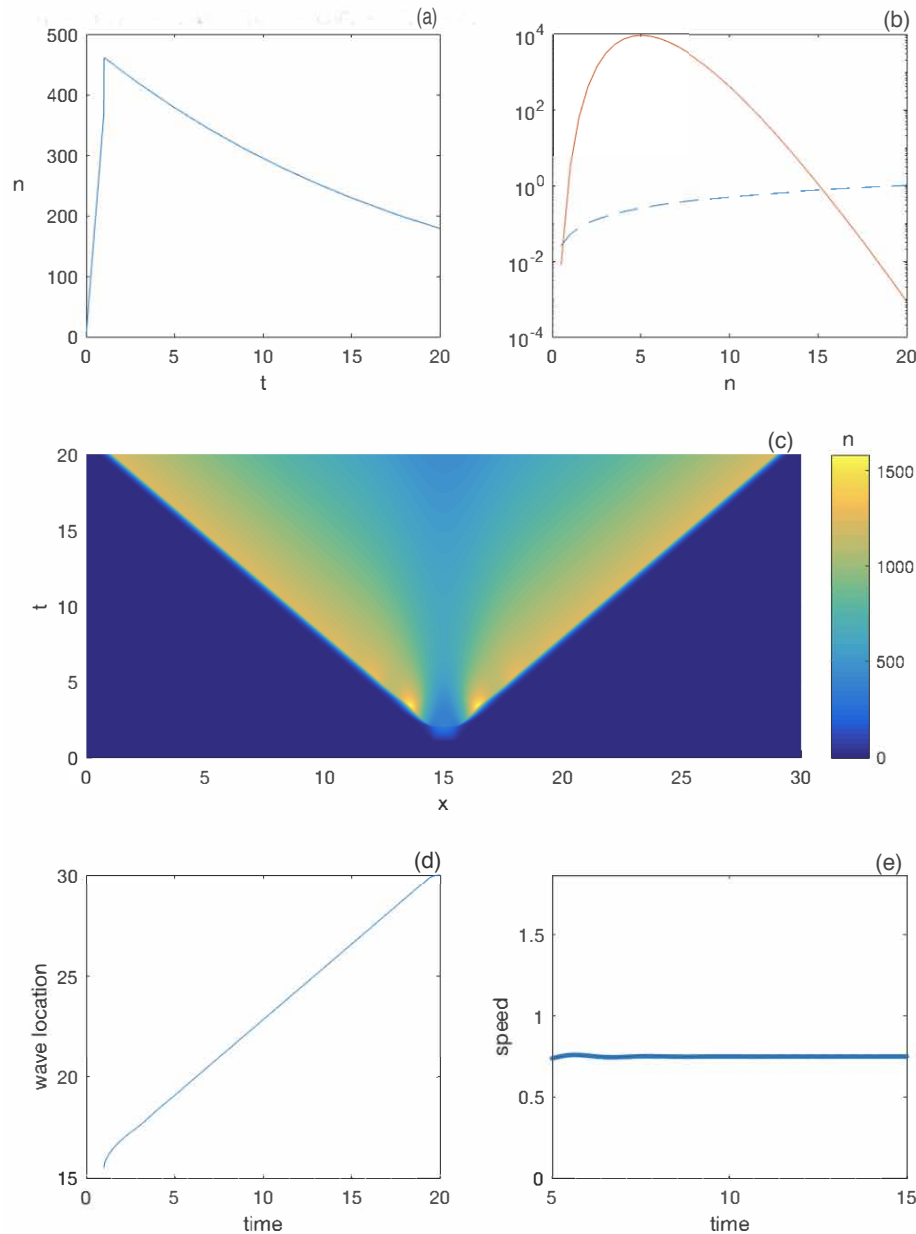
31

Figure S5: Simulation of model (Eq. 2 from SI Appendix), with $a_1 = 20$, $a_2 = 2$, $a_3 = 10$, $\mu = 0.05$, $\tau = 1$, and $D = 0.1$. For these parameters the *undelayed* ordinary differential equation (Eq. 2 from SI Appendix with $D = 0$ and $\tau = 0$) exhibits a strong Allee effect, evident by comparing the mortality rate (dashed blue line) to the reproduction rate (solid red curve) in panel (b) (note the logarithmic scale). With delays, the model without movement (Eq. 2 from SI Appendix with $D = 0$) exhibits decay to a stable equilibrium (a). The simulation of the partial functional differential equation (Eq. 2 from SI Appendix; initialized with $n = 2$ for $|x - 15| \leq 0.5$ and $0 \leq t \leq \tau$, and $n = 0$ otherwise) exhibits simple dynamics behind the invading fronts (c). High population densities behind the wave front push the invasion forward with a constant speed (d,e).
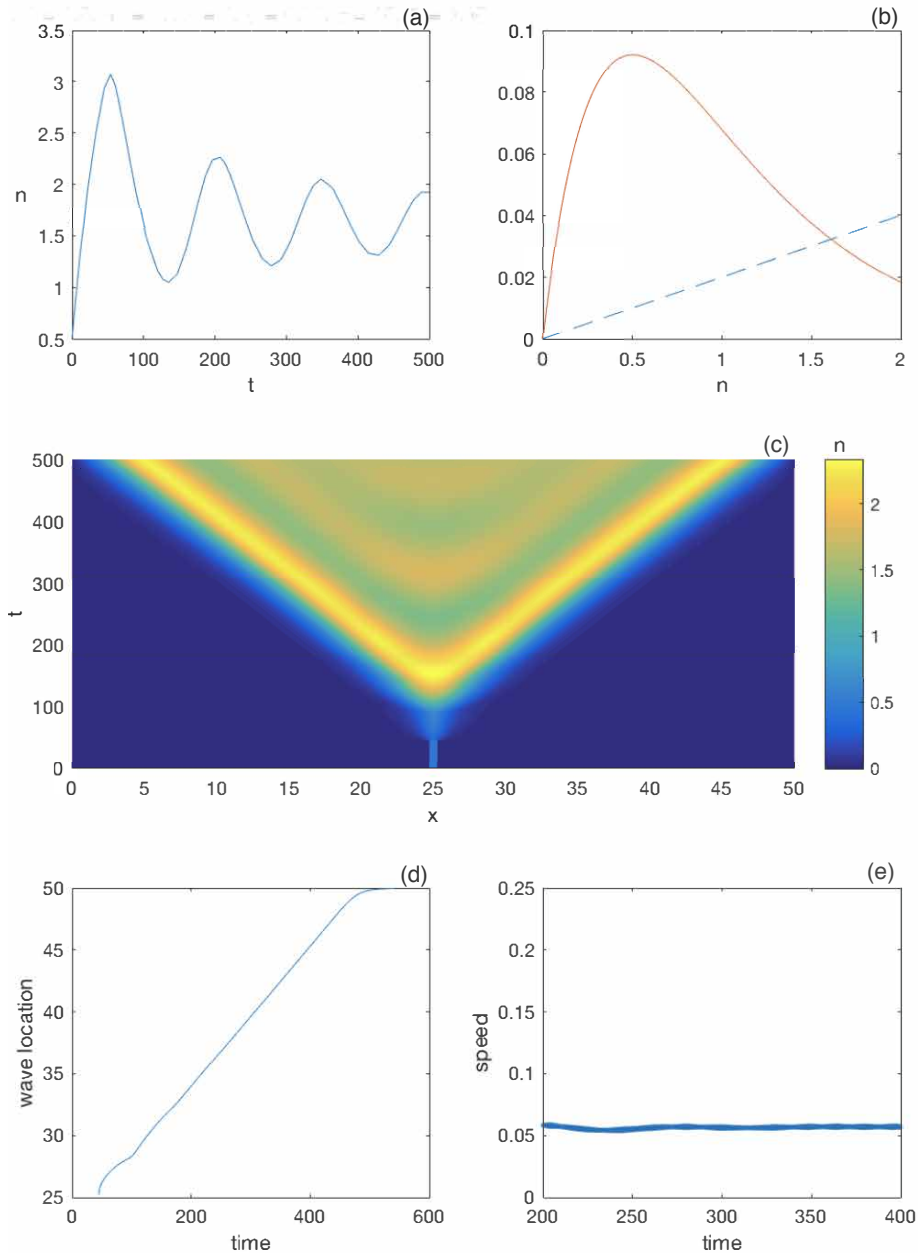
Figure S6: Simulation of model (Eq. 2 from SI Appendix) with $a_1 = 0.5$, $a_2 = 2$, $a_3 = 1$, $\mu = 0.02$, $\tau = 45$, and $D = 0.05$. For these parameters the *undelayed* ordinary differential equation (Eq. 2 from SI Appendix with $D = 0$ and $\tau = 0$) does not exhibit any Allee effect, evident by comparing the mortality rate (dashed blue line) to the reproduction rate (solid red curve) in panel (b) (note the arithmetic scale). With delays, the model without movement (Eq. 2 from SI Appendix with $D = 0$) produces oscillations in population density (a). The simulation of the partial functional differential equation (Eq. 2 from SI Appendix; initialized with $n = 0.5$ for $|x - 25| \leq 0.5$ and $0 \leq t \leq \tau$, and $n = 0$ otherwise) exhibits oscillatory dynamics behind the invading fronts (c); however, the wave is "pulled" by growth at low densities, so a constant invasion speed is achieved despite the fluctuations at high densities (d,e).
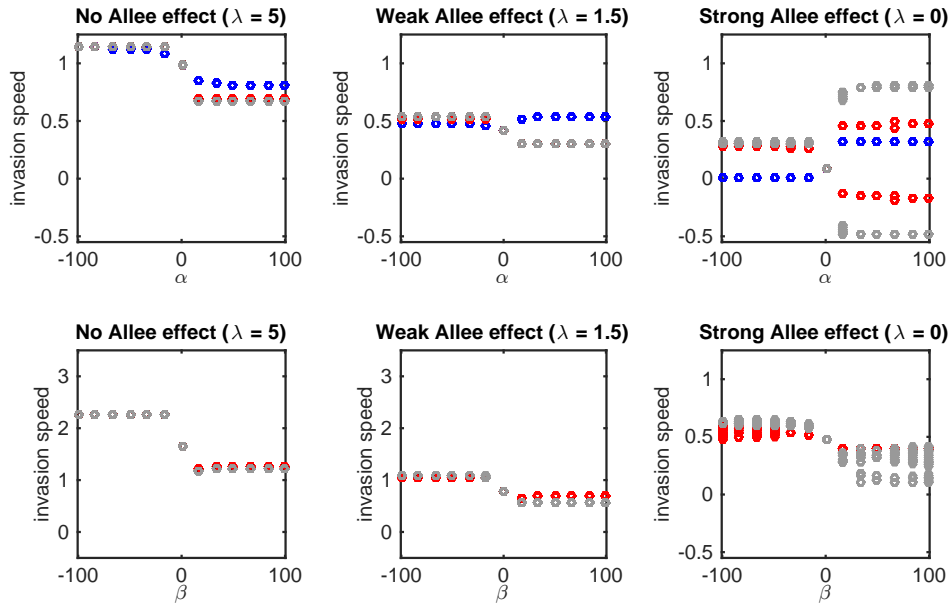
33

Figure S7: Bifurcation diagram indicating fluctuations in invasion speed across a range of Allee effect strength for the propensity Model – when density dependence alters dispersal propensity (a-c), and the distance model – when density dependence alters dispersal distance (d-f). Here, we also show a range of dispersal thresholds ($\hat{n}$) relative to Allee effect threshold used for these models in the text ($a = 0.2$), including $\hat{n} = 0.1 < a$ (blue circles), $\hat{n} = 0.7 > a$ (red circles), and $\hat{n} = 0.9 >> a$ (gray circles). All other parameters are the same as Fig. 2. Fluctuations in invasion speed only occur when Allee effects are strong, when the dispersal threshold is high, and when $\alpha > 0$ (propensity model (a-c)) or across a range of positive and negative $\beta's$ (distance model (d-f)).
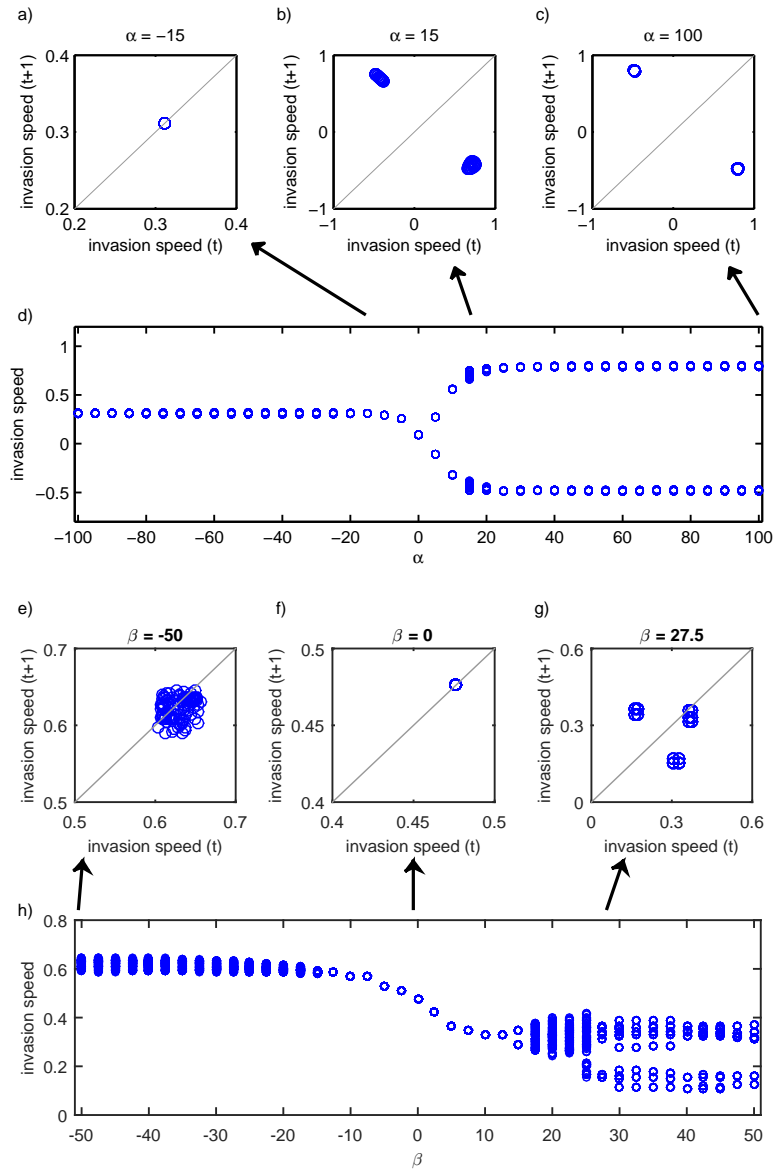
Figure S8: The periodicity of the invasion speed through time for the propensity model (Allee effects and density-dependent dispersal propensity; a-d) and distance model (Allee effects and density-dependent dispersal *distance*; e-h). In panels a-c and e-g, the wave position is plotted at time t vs time $t + 1$. In panels d and h, the range of invasion speeds represents the amplitude of fluctuations. For each parameter value, the invasion speed for the previous 100 time steps are plotted. When points appear as hollow points, the same invasion speed is being plotted over itself many times. For the propensity Model, when fluctuating, the wave speed is nearly always periodic across values of the Allee effect threshold a. At small values of α the invasion speed is constant (a), at small positive α the invasion speed fluctuates in a quasi-periodic fashion (b), and most positive α values, for example $\alpha = 100$ (c), the wave speed is periodic. Here, $\hat{n} = 0.9$, $\lambda = 0$, $\sigma^2 = 0.25$, $p_0 = 0.05$, $p_{max} = 1$, and $a = 0.2$. For the distance model, we demonstrate that the invasion speed appears to be more chaotic for some negative values of the density-dependent dispersal threshold (β) (e), is constant for some values of β (f), and has a quasi-periodic attractor for some positive values of β (g). Here, $\hat{n} = 0.9$, $\lambda = 0$, $\sigma_0^2 = 0.05$, $\sigma_{max}^2 = 1$, and $a = 0.2$.

SI Appendix

Here we construct a continuous-time model that we conjecture produces variable-speed invasions. We begin with a modification of a delay-differential equation model used by Gurney et al. (1) to study the dynamics of "Nicholson's blowflies:"

$$\frac{dn}{dt} = -\mu n + a_1 n(t - \tau)\, e^{-a_2 n(t-\tau)}. \tag{7}$$

In this model, n is the population size of mature animals, and τ is the maturation time. The change in the adult population size is due to constant per captia mortality (at rate μ) and recruitment of juveniles, born τ time units ago, into the adult class. The per captia birth rate at low density (a_1) is reduced (exponentially at the rate a_2) at larger population densities. This model produces large swings in adult population size when the maturation time is sufficiently large (1).

We modify the model (7) to include the potential for a strong Allee effect (when the parameter $a_3 > 1$) and to include the random movement of adults via diffusion:

$$\frac{\partial n}{\partial t} = -\mu n(x,t) + a_1 [n(x, t - \tau)]^{a_3}\, e^{-a_2\, n(x,t-\tau)} + D\frac{\partial^2 n(x,t)}{\partial x^2}. \tag{8}$$

Immature individuals are assumed to be sedentary.

The special case of model (8) with $a_3 = 1$ (without Allee effects) has been thoroughly studied (see, e.g., Lin et al. (2) and Solar and Trofimchuk (3) and references therein). The dynamics of this model in this case can be quite complex behind the leading invasion front, but, for biologically realistic initial conditions solutions, solutions exhibit an asymptotically constant spreading speed.

Much less is know about the dynamics of equation (8) when $a_3 > 1$, but the model would seem to have the features necessary to generate variable invasion speed.

36

531 Density-dependent reproduction, along with the maturation time delay, induce popu-

532 lation fluctuations at high density, and the Allee effect should generate a pushed wave.

533 Our numerical simulations suggest that this is indeed the case (Fig. S4). When, in

534 contrast, the population dynamics converge to an equilibrium point behind the inva-

535 sion front, the invasion speed is eventually constant, even in the presence of an Allee

536 effect (Fig. S5). In the absence of Allee effects ($a_3 = 1$), simulations of the model

537 (8) produce constant speed invasions (Fig. S6), even if there are oscillatory dynamics

538 behind the front, in agreement with prior theory.

References

540 [1] Gurney, W.S.C., Blythe, S. P. and Nisbet, R. M. 1980. Nicholson's blowflies re-

541 visited. *Nature* **287**:17–21.

542 [2] Lin, C-K., Lin, C-T, Lin, Y, and Mei, M. 2014. Exponential stability of non-

543 monotone traveling waves for Nicholson's blowflies equation. *SIAM Journal on*

544 *Mathematical Analysis* **46**:1053–1084.

545 [3] Solar, A. and Trofimchuk, S. 2015. Asymptotic convergence to pushed wavefronts

546 in a monostable equation with delayed reaction. *Nonlinearity* **28**:2027–2052.